

Fabrication and Properties of Poly(L-lactide) Nanofibers via Blend Sea-Island Melt Spinning

Xiuqin Zhang, Gaoling Jin, Wenjuan Ma, Lingyan Meng, Huihui Yin, Zhiguo Zhu, Zhenfeng Dong, Rui Wang

Department of Materials Science and Engineering, Beijing Institute of Fashion Technology, Beijing 100029, China

Correspondence to: R. Wang (E-mail: clywangrui@bift.edu.cn)

ABSTRACT: Poly(L-lactide) (PLLA) nanofibers were prepared by melt extrusion of immiscible blends of PLLA/low density polyethylene (LDPE) and subsequent removal of the LDPE matrix from the blend fibers. The effect of blends composition and draw ratio on the phase structure of the blend fibers, crystallization, mechanical properties, and the diameter of the PLLA nanofibers was investigated. It is found that the diameter of the PLLA phase gradually increases with the increase of PLLA content. With the variation of PLLA content from 50 to 60 wt %, the average diameter of acquired PLLA nanofibers changes from 119 to 153 nm under the draw ratio of 1.5. When further increasing the content of PLLA to 65%, it is difficult to acquire PLLA nanofibers due to the poor dissolving properties between PLLA and LDPE components. Oriented PLLA nanofibers with the average diameter of 92 nm can be fabricated from PLLA/LDPE (50/50, wt %) blends under the draw ratio of 2. The present results suggest that it is possible to acquire polymer nanofibers with high output using blend sea-island melt spinning. © 2014 Wiley Periodicals, Inc. *J. Appl. Polym. Sci.* **2015**, *132*, 41228.

KEYWORDS: blends; fibers; manufacturing; morphology; phase behavior

Received 4 May 2014; accepted 27 June 2014

DOI: 10.1002/app.41228

INTRODUCTION

Poly(L-lactide) (PLLA) is produced from renewable biomass such as corn or biological waste materials. It is a biodegradable and biocompatible polymer and exhibits reasonable mechanical properties. The fibers made of PLLA have the advantages of both natural and synthetic fibers, such as excellent permeability and moisture absorption, comfortability, nontoxicity, biodegradability, and biocompatibility, etc., which can be widely used in high-grade clothing fabrics, textile materials, and biomedical fields.¹ The size of the PLLA fibers plays an important role in the properties of final materials. A smaller diameter leads to larger surface area per unit mass and smaller pore size, which is useful in filtration application and tissue engineering.^{2,3} For example, if the diameter of PLLA fiber decreases from 22 μm to 880 nm, the pore diameter of nonwovens composed of nanofibers would decrease from 66 μm to 8 μm .⁴ For this reason, preparation and properties of PLLA nanofibers have attracted great attention.

Electrospinning is the most popular method in preparation of PLLA nanofibers, including solution and melt electrospinning.^{3,5–7} Solution electrospinning can prepare polymer fibers with diameters in the range from several micrometers down to 100 nm. But several major drawbacks are encountered in solution electrospinning. The production efficiency is low and the

prepared nanofibers have low crystallinity and orientation.^{5,7,8} Melt electrospinning has higher fiber production rate, but it is difficult to obtain PLLA nanofibers due to the high viscosity, low electron conductivity, and die swelling of polymer melts.⁸ The minimum diameter of PLLA fibers produced by this method could not be smaller than 800 nm.⁶ In addition, researchers reported a method of producing PLLA nanofibers by means of a carbon dioxide (CO₂) laser supersonic drawing. PLLA nanofibers with a diameter of 132 nm were obtained, while the velocity of as-spun fibers is about 0.1 m/min and thus the efficiency is low.

In recent years, the blend sea-island melt spinning also provide a method to produce polymer nanofibers. The principle is to choose two kinds of partially miscible or immiscible thermoplastic polymers, mixing and melt spinning by triaxial spinning machine. By regulating the viscosity ratio of the blends, the composition and spinning conditions, blend fibers with sea-island structure can be fabricated. After dissolving and removing the sea phase of the blend fibers, the nanofibers are obtained.^{9,10} By using this method, polypropylene (PP),^{11–14} poly(trimethylene terephthalate) (PTT)^{15,16} and poly(butylene terephthalate) (PBT)¹⁷ nanofibers have already been obtained successfully. For example, Li et al. reported the preparation of PET, PTT, and PBT nanofibers from PET/cellulose acetate

butyrate (CAB), PTT/CAB, PBT/CAB immiscible blends by *in situ* microfibrillar formation during the melt extruding process.¹⁸ The average diameters of the obtained PET, PTT, and PBT nanofibers are nearly 200 nm by controlling the processing conditions.¹⁸ Fallahi et al. obtained PP and PA6 nanofibers with the diameter from 200 to 1000 nm by regulating the processing conditions.¹³ These results suggest that the method of blend sea-island melt spinning is suitable to produce polymer nanofibers. Moreover, the technology of melt-spinning is well-developed and the equipment is relatively simple, therefore, the method of the sea-island melting spinning is promising. However, preparation of PLLA nanofibers using this method has not been reported yet.

As the precursor of the nanofibers, the island phase decides directly the output of nanofibers. Previous studies provide some information on the preparation of polymer nanofibers at low island contents (<50%) via blend sea-island melt spinning.^{11–18} Because the sea phase would be removed by solvents, basically, the higher the fraction of island phase, the higher the production efficiency of nanofibers. Therefore, the purpose of this study is to explore the morphology development of PLLA/low density polyethylene (LDPE) immiscible blends with high fraction of island phase during processing. PLLA nanofibers are prepared using this method and the properties of nanofibers are investigated.

EXPERIMENTAL

Materials

Commercial grade PLLA (6202D) was purchased from Natureworks and the melt flow index is 24.7 kg/10min (210°C/2.16 kg). LDPE (1I50A) was supplied by China Petrochemical Corporation and the melt flow index is 38.0 kg/10 min (190°C/2.16 kg).

Preparation

PLLA was dried at 70°C in a vacuum oven for more than 15 h. The blending and spinning of PLLA and LDPE were carried out by a one-step method. After mixing PLLA with LDPE in a solid mixer, the mixture pellets were fed into a single-screw extruder (diameter = 30 mm, $L/D = 25$) with a spinneret containing 24 orifices with 0.3 mm diameter. The five temperature zones of the extruder was set at 130, 190, 200, 205, and 210°C at the feed, metering, melt-blending, die and spinneret sections, respectively. PLLA/LDPE as-spun fibers were collected at a take-up speed of 400 m/min, and followed by one-step thermodrawing of 1.5–2 times elongation at 80°C and a subsequent thermo-fixing process at 90°C (designated as “PLLA/LDPE drawn fibers”). PLLA/LDPE samples without coiling were also collected as the control samples, coded as “PLLA/LDPE blends”.

Measurement and Characterization

To clearly see the morphology, the blends were fractured in liquid nitrogen and etched with methylene dichloride at 95°C for 1 min to remove the PLLA component. The resulting blend fibers were immersed in xylene at 95°C for 60 min to remove LDPE. The surfaces of the blends and fibers were observed using a JSM-6700F JEOL scanning electron microscope (SEM). All SEM specimens were coated with gold of ~5-nm-thick to avoid charging; thereby, improving image quality. One hundred of fibers were counted in calculating the number average and

distribution of nanofiber diameters. Number average diameters of nanofibers were calculated as follows.

$$D_N = \frac{\sum N_i D_i}{\sum N_i} \quad (1)$$

where D_N is the number averaged diameter, N_i is the number of nanofibrils with a diameter of D_i .

WAXS profiles between 5° and 40° were collected using a Rigaku D/MAX-RB X-ray diffractometer with CuK α radiation ($\lambda = 1.54 \text{ \AA}$) at a generator voltage of 40 kV and a generator current of 50 mA.

The thermal behavior of nanofibers was determined by DSC (DSC6200, Seiko) using 6.00 mg samples at a heating rate of 10°C/min under nitrogen atmosphere. The crystallinity of PLLA nanofibers is calculated by $X_c = \Delta H / \Delta H_0 \times 100\%$, in which ΔH (J/g) is PLLA melting enthalpy, ΔH_0 is the melting enthalpy corresponding to 100% crystalline PLLA of 93.6 J/g.¹⁹

The infrared (IR) spectra of PLLA/LDPE blend fibers were accumulated using a Bruker EQUINOX 55 spectrometer with a resolution of 4 cm^{-1} and 32 scans. In order to characterize the orientation of the fibers, the IR spectra with polarized radiation parallel ($A_{||}$) and perpendicular (A_{\perp}) to the fiber axis were measured. The dichroic ratio (D) was used to describe the orientation of macromolecular chains of every component in blend fibers.

$$D = A_{||} / A_{\perp} \quad (2)$$

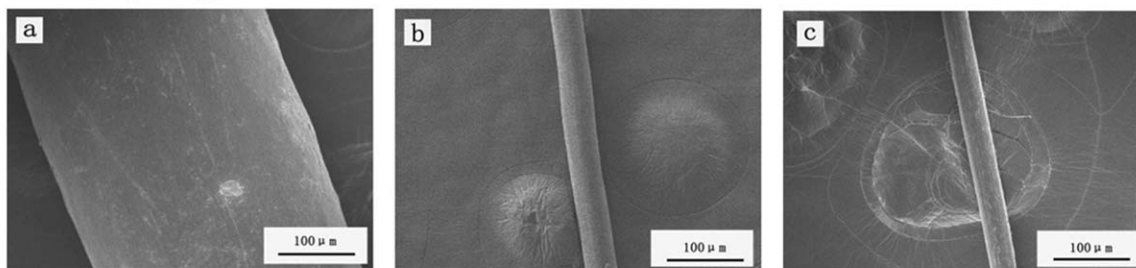
The stretching properties of the fibers were measured on a tensile testing machine (YG004N). The stretching speed is 40 mm/min.

RESULTS AND DISCUSSION

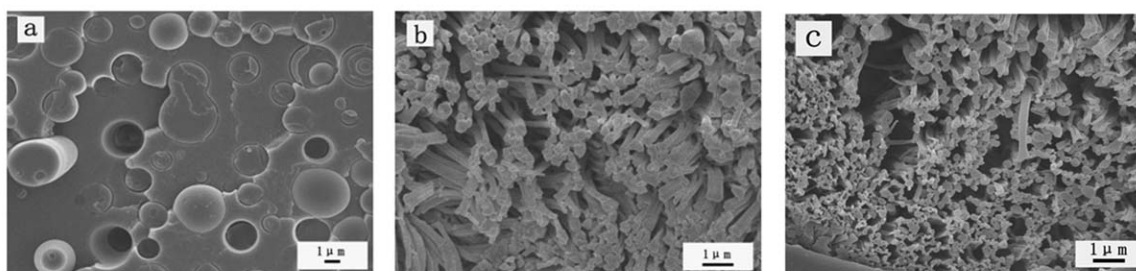
Fabrication of PLLA Nanofibers and Morphology

The formation of PLLA nanofibers via blend sea-island melt spinning includes the processes of blending, extruding, spinning, drawing, and dissolution. Morphology development in different stages is shown in Figure 1. PLLA/LDPE blends were collected without coiling; therefore, the diameter of the island phases is large [Figure 1(a)]. When the fibers are collected at a take-up speed of 400 m/min, as a result of the effect of take-up stress and temperature, the island phases were deformed to form microfibrils from rod-like phases [Figure 1(b)]. Further drawing the as-spun PLLA/LDPE fibers, the diameter of PLLA islands decreases and PLLA nanofibers were obtained after removing the LDPE matrix by xylene [Figure 1(c)]. According to the SEM images of PLLA island phases in blend fibers, a large number of PLLA filaments are evenly distributed in the cross sections of PLLA/LDPE fibers, which favors the preparation of PLLA nanofibers with uniform size. In principle, the key points for the method of blend sea-island melt spinning is to precisely regulate the phase morphology between the matrix and dispersed phases, and control the diameter of island microfibrils at nanoscale as well as maintain good stripping property. Many factors influence the structure formation of PLLA/LDPE blends including blend ratio, compatilizer, spinning condition, etc. Herein, we explore the effect of blend ratio and draw ratio

Surface morphology of PLLA/LDPE



Morphology of PLLA island phases



Morphology of PLLA after removing LDPE

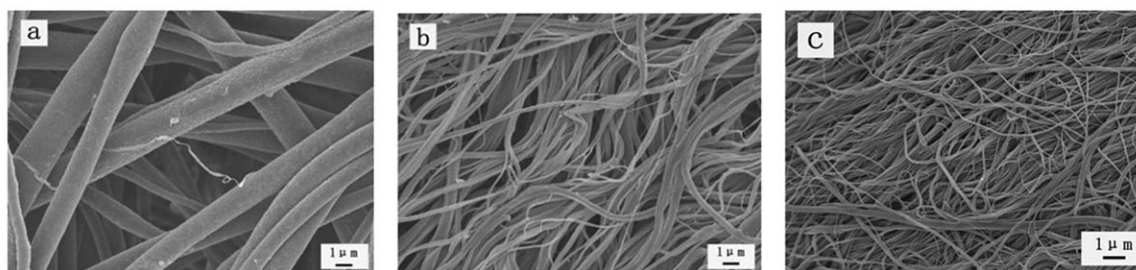


Figure 1. SEM images of different surfaces in the formation process of PLLA nanofibers. (The blend ratio of PLLA/LDPE is 50/50, wt %. The take-up speed is 400 m/min and the draw ratio is 2.) (a) PLLA/LDPE blends, (b) PLLA/LDPE as-spun fibers, (c) PLLA/LDPE drawn fibers.

on the formation and properties of PLLA/LDPE blend fibers and PLLA nanofibers.

Effect of Blend Ratio

Blend ratio plays a crucial role in controlling the microstructure and phase size of polymer blends during blend sea-island melt spinning.^{17,20} Figure 2 shows the SEM images of fracture surface of PLLA/LDPE blends with different blend ratios after etching PLLA. A typical sea-island two-phase structure is observed. With the increase of PLLA fraction, the size of island phase increases due to the collision of PLLA droplets, and the uniformity of diameter distribution of PLLA phase decreases. To obtain quantitative information, the diameter distribution and average domain sizes of PLLA phases were calculated by analyzing SEM images with an image analysis software image-Pro Plus, as shown in Figure 3. The cross-section of PLLA dispersed domains is in the range of 1–3 μm . At the blend ratio of PLLA/LDPE of 65/35, the size of PLLA phases is bigger than that in other blends with lower PLLA content.

Figure 4 presents the SEM images of PLLA nanofibers after removing LDPE matrix from the PLLA/LDPE drawn fibers. The drawn fibers were obtained by stretching the as-spun fibers with

the draw ratio of 1.5. At the blend ratio of PLLA/LDPE 50/50, 55/45, and 60/40, PLLA nanofibers can be obtained after the removal of the LDPE matrix. Adhesion of nanofibers becomes obvious with the increase of PLLA content. When the content of PLLA is 65 wt %, PLLA nanofibers cannot be fabricated due to the fact that the LDPE matrix cannot be removed completely under the wrapping of PLLA phases. Figure 5 shows the diameter distribution and the average diameter of PLLA nanofibers produced from PLLA/LDPE drawn fibers with the draw ratio of 1.5. With the increase of PLLA fraction from 50 to 60 wt %, the average diameter of PLLA nanofibers increases from 119 to 153 nm. Furthermore, the diameter distributions of PLLA nanofibers became broader. The variation regulation of PLLA nanofibers is in consistency with that of PLLA island phases in blends. This is mainly caused by the higher possibility of coalescence of PLLA with the increase of PLLA component.

The formation mechanism of dispersed phase during melt blending of polymers has been studied extensively. For the same polymer blends, there are two factors determining the sea-island morphology of blends: the viscosity ratio $p = \eta_d/\eta_m$ (η_d , viscosity of the dispersed phase; η_m , viscosity of the matrix phase) and blend composition.^{21–23} The component with high viscosity

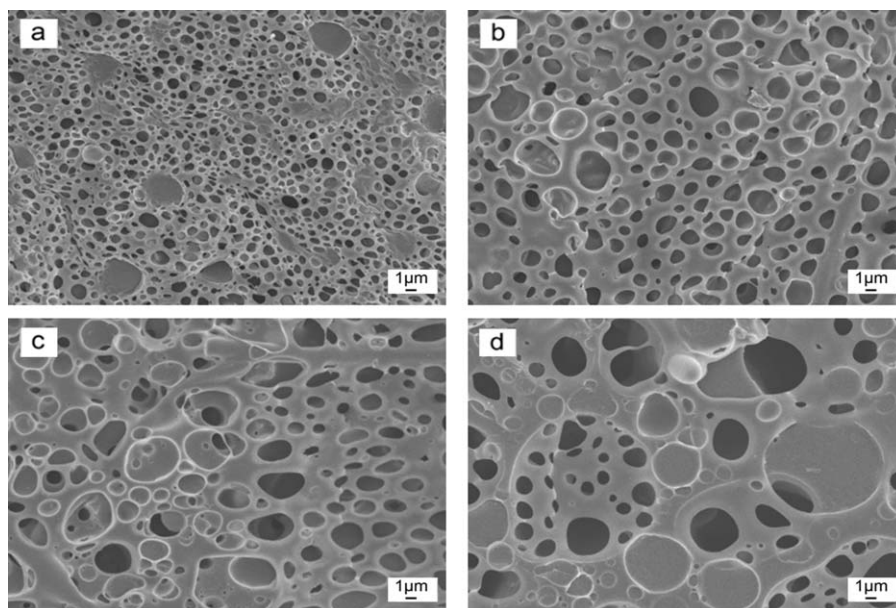


Figure 2. SEM images of fracture surface of PLLA/LDPE blends after removing PLLA. (a) 50/50, (b) 55/45, (c) 60/40, (d) 65/35.

is prone to form the dispersed phase. If one wants to increase the content of island phase, it is necessary to increase the viscosity of island component or decrease the viscosity of the sea component. Figure 6 shows the viscosity ratio of PLLA/LDPE at different shear rates and processing temperatures. In the whole range of explored experimental conditions, the viscosity ratio is higher than 1, indicating that PLLA tends to form the island phase. PLLA can still form the island phase in PLLA/LDPE blends with 60 wt % PLLA, which is beneficial to improve the

output of nanofibers. On the other hand, the dispersed particle size is proportional to $p^{0.84}$ when $p > 1$ or $p^{-0.84}$ when $p < 1$. Blends with a viscosity ratio close to unity would form the smallest dispersed phase particles. For acquiring the island fibers with smaller size, the viscosity ratio should be considered combining the output and the size of island fibers. In our case, PLLA fibers with the size of 119–153 nm were obtained at appropriate processing conditions when the fraction of PLLA components in blends was equal to or higher than 50 wt %.

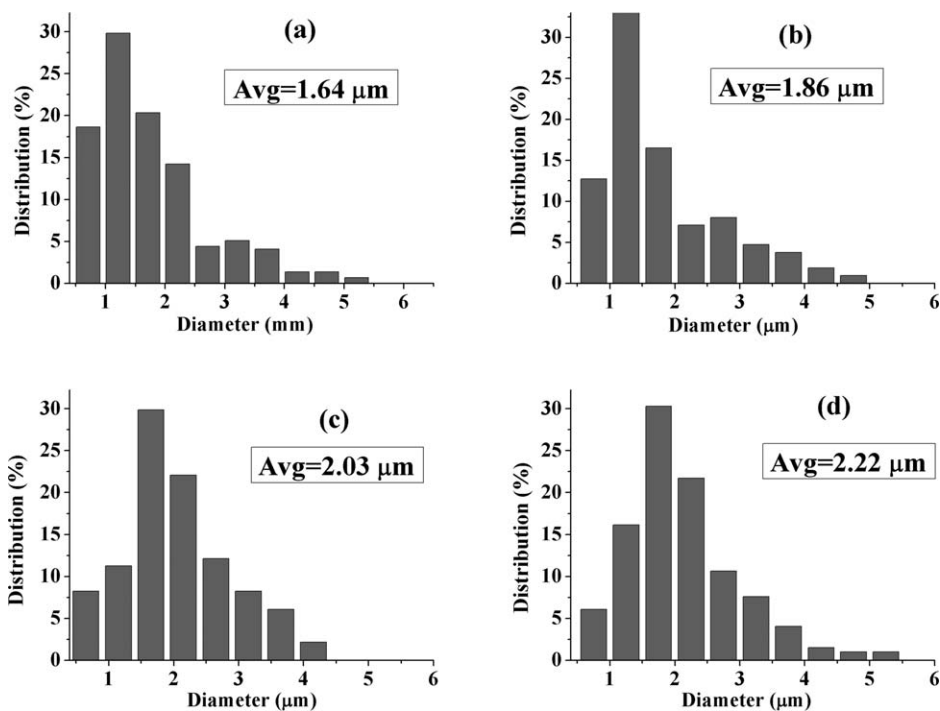


Figure 3. Diameter distribution of PLLA phase in PLLA/LDPE blends. (a) 50/50, (b) 55/45, (c) 60/40, (d) 65/35.

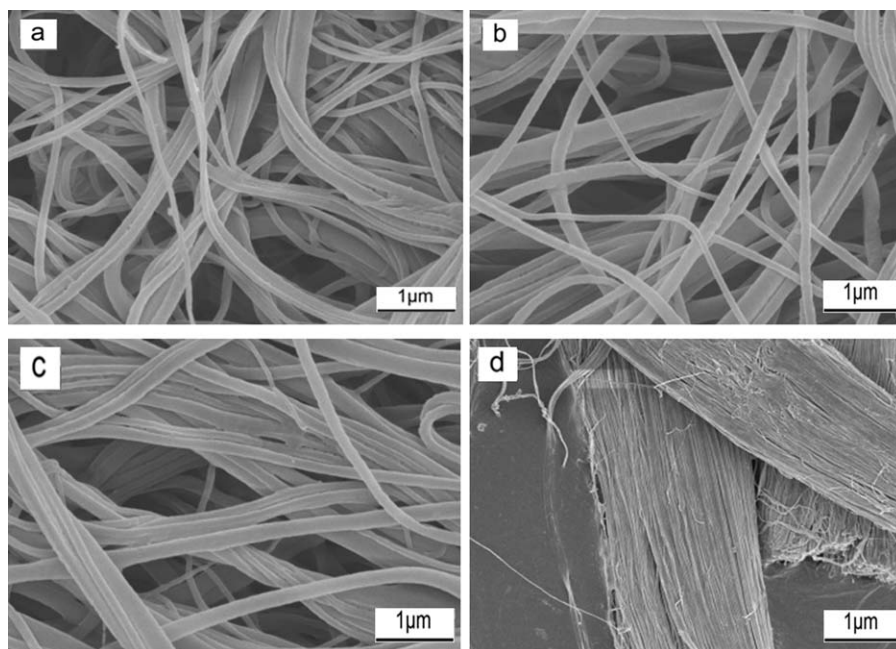


Figure 4. Morphology of PLLA nanofibers extracted from PLLA/LDPE drawn fibers (a) 50/50, (b) 55/45, (c) 60/40, (d) 65/35.

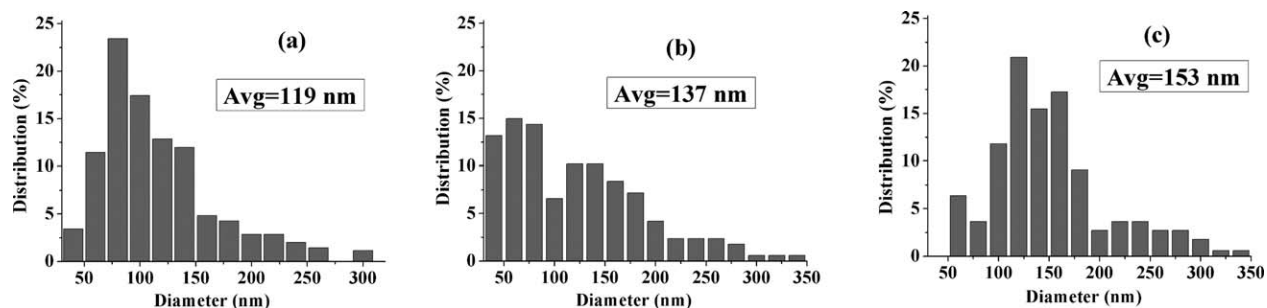


Figure 5. Average diameter and distribution of PLLA nanofibers. (a) 50/50, (b) 55/45, (c) 60/40.

Effect of Draw Ratio

The drawing favors the formation of microfibrils from the deformation of the dispersed phases in an immiscible blends, thus the draw ratio is also an important factor in controlling the size of island fibers. Figure 7 shows the SEM images of PLLA nanofibers obtained from PLLA/LDPE (50/50, wt %) blend fibers with different draw ratios. With the increase of draw ratio, PLLA diameter has an obvious decrease from 119 to 92 nm. Meanwhile, diameter distribution is narrower from 40–300 nm to 40–280 nm (Figure 8). Higher draw ratio provides higher drawing deformation to the polymer as-spun fibers, which facilitates the decrease of size of island fibers, and simultaneously improve the orientation and crystallization of fibers.

Properties of PLLA Nanofibers

Many studies have shown that PLLA can crystallize in α -, β -, and γ - forms.^{24–27} Among these forms, α form is the most common and stable form, which can be often acquired by melting or solution crystallization. Figure 9 shows the XRD profiles of PLLA nanofibers. The diffraction peaks at $2\theta = 16.7^\circ$ and 18.9° are assigned to the reflections from (200)/(110) and (203)

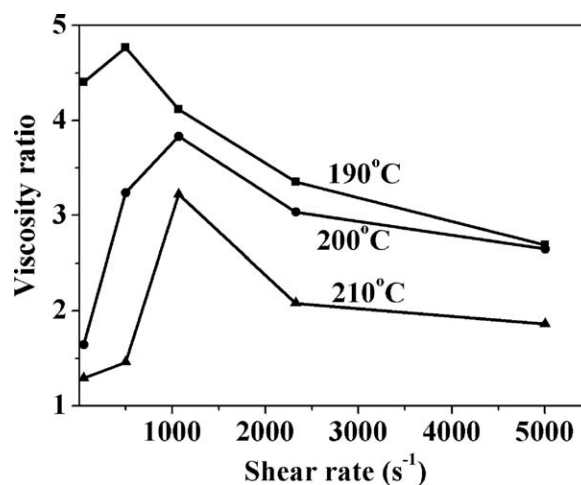


Figure 6. Viscosity ratio variation of PLLA/LDPE as a function of shear rate at different temperatures.

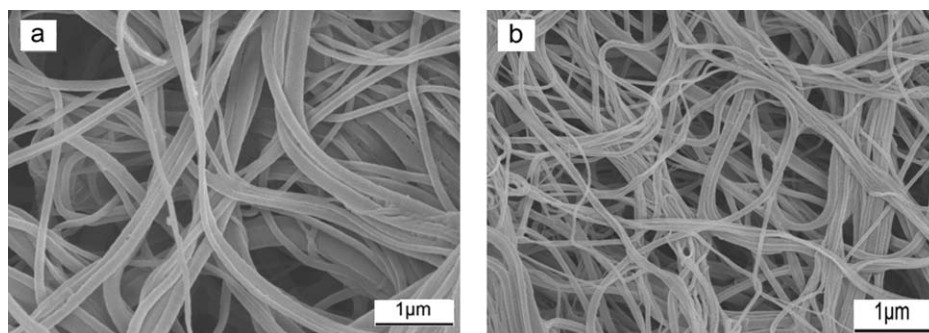


Figure 7. SEM images of PLLA nanofibers obtained from PLLA/LDPE (50/50, wt %) blend fibers with different draw ratios (a) 1.5, (b) 2.0.

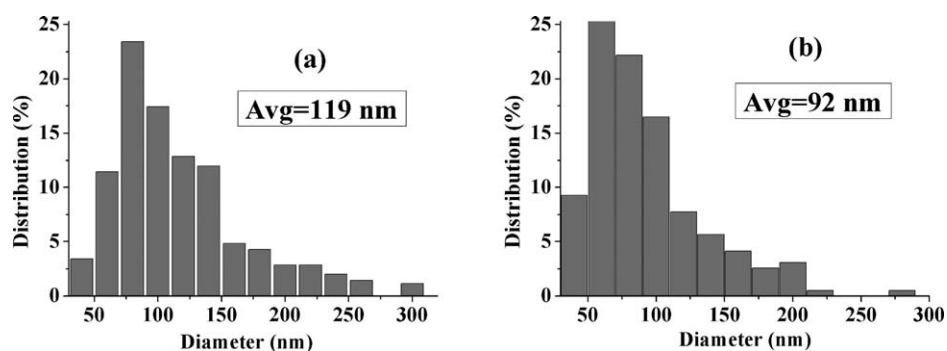


Figure 8. Diameter distribution of PLLA nanofibers obtained from PLLA/LDPE (50/50, wt %) blend fibers with different draw ratios (a) 1.5, (b) 2.0.

planes of α -form of PLLA, respectively. It can be seen that the PLLA nanofibers obtained from PLLA/LDPE blend fibers with different draw ratio form the stable α crystal form, which is in favor of the stability of subsequent application. The crystallinity calculated by DSC results shows the slight increase from 60% to 62% with the variation of draw ratio from 1.5 to 2.

The dichroic ratio of IR spectra provides an access to the degree of orientation for the crystalline and the amorphous region.

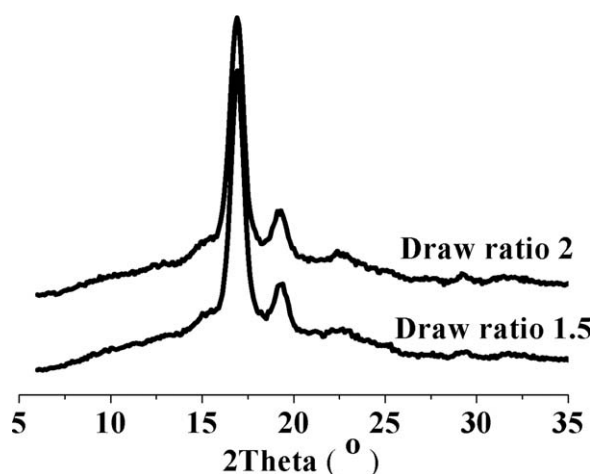


Figure 9. XRD curves of PLLA nanofibers obtained from PLLA/LDPE (50/50, wt %) blend fibers with different draw ratios.

Figure 10 shows the polarizing FTIR spectra of PLLA blend fibers with different draw ratios. The band of 958 cm^{-1} , arising from the coupling of C—C backbone stretching and the CH_3 rocking mode, is assigned to the amorphous phase of PLLA. The band at 1752 cm^{-1} , arising from the C=O stretching modes, is assigned to the crystalline phase of PLLA.^{28,29} The calculated dichroism ratio of 958 cm^{-1} and 1752 cm^{-1} are shown in Table I. It can be seen that the degree of orientation of PLLA

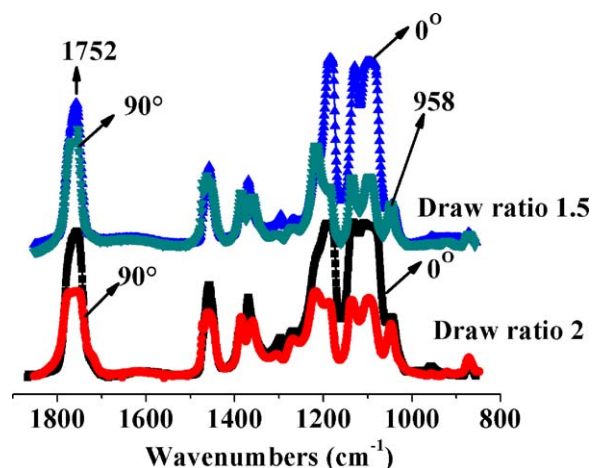


Figure 10. Polarizing FTIR spectra of PLLA/LDPE (50/50, wt %) blend fibers with different draw ratios. [Color figure can be viewed in the online issue, which is available at wileyonlinelibrary.com.]

Table I. IR Dichroism Ratio of PLLA/LDPE (50/50, wt %) Blend Fibers

IR bands (cm ⁻¹)	Draw ratio	
	1.5	2.0
1752	1.19	1.70
958	2.52	2.93

Table II. Mechanical Properties of PLLA/LDPE (50/50, wt %) Blend Fibers

Draw ratio	Diameter (μm)	Tensile strain (%)	Breaking strength (MPa)
1.5	35.4	44.0 ± 3	200 ± 16
2.0	30.0	30.0 ± 3	223 ± 21

nanofibers in blends increases with the increase of draw ratios. The slight increase of crystallinity and orientation with the variation of draw ratio from 1.5 to 2 results in the slight improvement of the mechanical properties, as show in Table II.

CONCLUSIONS

In the present work, PLLA nanofibers were prepared by blend sea-island melt spinning method. The diameter of the PLLA nanofibers can be controlled by adjusting the viscosity ratio and processing conditions. With the variation of PLLA content from 50 to 60 wt % in the blends, the average diameter of acquired PLLA nanofibers changes from 119 to 153 nm. Further increasing the content of PLLA to 65%, it is difficult to fabricate PLLA nanofibers due to the bad dissolving properties between PLLA and LDPE components. The PLLA nanofibers crystallize into the stable α -form with the crystallinity around 60%, indicating that the nanofibers would have good shape stability during application. As revealed by polarized IR, the polymer chains in the nanofibers are highly oriented. These results demonstrated that this method is promising both in nanofiber properties and production output. It must be noted that the solvent and sea phase can be totally recycled and reused, therefore environmental protection can be achieved.

ACKNOWLEDGMENTS

This work was supported by Beijing Nova Program (2011016), New Century Excellent Talents in University (NCET-12-0601) and Natural Science Foundations (KZ201310012014 and 11179031).

REFERENCES

- Gupta, B.; Revagade, N.; Hilborn, J. *Prog. Polym. Sci.* **2007**, *32*, 455.

- Lee, J. Y.; Bashur, C. A.; Goldstein, A. S.; Schmidt, C. E. *Bio-materials* **2009**, *30*, 4325.
- Li, D. P.; Frey, M. W.; Baeumner, A. J. *J. Membr. Sci.* **2006**, *279*, 354.
- Li, Y.; Joo, C. W. *J. Appl. Polym. Sci.* **2012**, *126*, E252.
- Zhang, X.; Nakagawa, R.; Chan, K. H. K.; Kotaki, M. *Macromolecules* **2012**, *45*, 5494.
- Zhou, H.; Green, T. B.; Joo, Y. L. *Polymer* **2006**, *47*, 7497.
- Bognitzki, M.; Czado, W.; Frese, T.; Schaper, A.; Hellwig, M.; Steinhart, M.; Greiner, A.; Wendorff, J. H. *Adv. Mater.* **2001**, *13*, 70.
- Lyons, J.; Li, C.; Ko, F. *Polymer* **2004**, *45*, 7597.
- Wang, D.; Sun, G.; Chiou, B.-S. *Macromol. Mater. Eng.* **2007**, *292*, 407.
- Wang, D.; Sun, G. *Eur. Polym. J.* **2007**, *43*, 3587.
- Xue, C. H.; Wang, D.; Xiang, B.; Chiou, B.-S.; Sun, G. *J. Polym. Res.* **2011**, *18*, 1947.
- Xue, C. H.; Wang, D.; Xiang, B.; Chiou, B.-S.; Sun, G. *J. Polym. Sci. Part B-Polym. Phys.* **2010**, *48*, 921.
- Fallahi, E.; Barmar, M.; Kish, M. H. *J. Appl. Polym. Sci.* **2008**, *108*, 1473.
- Wang, D.; Sun, G.; Chiou, B.-S.; Hinestroza, J. P. *Polym. Eng. Sci.* **2007**, *47*, 1865.
- Wang, D.; Sun, G. *J. Appl. Polym. Sci.* **2011**, *119*, 2302.
- Xue, C. H.; Wang, D.; Xiang, B.; Chiou, B.-S.; Sun, G. *Mater. Chem. Phys.* **2010**, *124*, 48.
- Li, M.; Xiao, R.; Sun, G. *Polym. Eng. Sci.* **2011**, *51*, 835.
- Li, M.; Xiao, R.; Sun, G. *J. Appl. Polym. Sci.* **2012**, *124*, 28.
- Fischer, E. W.; Sterzel, H. J.; Wegner, G. *Kolloid-Zeitschrift and Zeitschrift Fur Polymere* **1973**, *251*, 980.
- Li, M. F.; Xiao, R.; Sun, G. *J. Mater. Sci.* **2011**, *46*, 4524.
- Wu, S. *Polym. Eng. Sci.* **1987**, *27*, 335.
- Favis, B. D.; Willis, J. M. *J. Polym. Sci. Part B-Polym. Phys.* **1990**, *28*, 2259.
- Favis, B. D.; Therrien, D. *Polymer* **1991**, *32*, 1474.
- Sawai, D.; Takahashi, K.; Imamura, T.; Nakamura, K.; Kanamoto, T.; Hyon, S. H. *J. Polym. Sci. Part B-Polym. Phys.* **2002**, *40*, 95.
- Sawai, D.; Takahashi, K.; Sasashige, A.; Kanamoto, T.; Hyon, S. H. *Macromolecules* **2003**, *36*, 3601.
- Sawai, D.; Yokoyama, T.; Kanamoto, T.; Sungil, M.; Hyon, S. H.; Myasnikova, L. P. *Macromol. Symp.* **2006**, *242*, 93.
- Takahashi, K.; Sawai, D.; Yokoyama, T.; Kanamoto, T.; Hyon, S. H. *Polymer* **2004**, *45*, 4969.
- Furukawa, T.; Sato, H.; Murakami, R.; Zhang, J.; Duan, Y.-X.; Noda, I.; Ochiai, S.; Ozaki, Y. *Macromolecules* **2005**, *38*, 6445.
- Krikorian, V.; Pochan, D. *J. Macromolecules* **2001**, *38*, 6520.